**Proceedings of the ASME 2017 36th International Conference on Ocean, Offshore and Arctic Engineering**
**OMAE2017**
**June 25-30, 2017, Trondheim, Norway**

# OMAE2017-62233

# THE EFFECTS OF SURFACE WAVES AND SUBMERGENCE ON THE PERFORMANCE AND LOADING OF A TIDAL TURBINE

**Xiaoxian Guo** *
State Key Laboratory of Ocean Engineering
Shanghai Jiao Tong University
Shanghai, 200240, China
Email: xiaoxguo@sjtu.edu.cn

**Zhen Gao**
Department of Marine Technology
Norwegian University of Science and Technology
Trondheim, 7491, Norway
Email: zhen.gao@ntnu.no

**Jianmin Yang**
State Key Laboratory of Ocean Engineering
Shanghai Jiao Tong University
Shanghai, 200240, China
Email: jmyang@sjtu.edu.cn

**Torgeir Moan**
Center for Ships & Ocean Structures
Department of Marine Technology
Norwegian University of Science and Technology
Trondheim, 7491, Norway
Email: torgeir.moan@ntnu.no

**Haining Lu**
State Key Laboratory of Ocean Engineering
Shanghai, 200240, China
Email: haining@sjtu.edu.cn

**Xin Li**
State Key Laboratory of Ocean Engineering
Shanghai, 200240, China
Email: lixin@sjtu.edu.cn

**Wenyue Lu**
State Key Laboratory of Ocean Engineering
Shanghai, 200240, China
Email: lwy_qiye@sjtu.edu.cn

## ABSTRACT

Tidal energy has the advantages of high predictability, high energy density, and limited environmental impacts. As tidal turbines are expected to be used in the most energetic waters where there might be significant waves, the assessment of unsteady hydrodynamic load due to surface waves is of great concern. The objective of this paper is to assess the effects of surface waves and submergence of the turbine on the power performance and loads of a tidal turbine by experimental approach. The experiments on a $1:25$th model tidal turbine were carried out in a towing tank. A wide range of regular waves with periods from 1.0 s to 3.0 s at model scale were generated. Different submergence conditions were considered to investigate the effects of the presence of free surface. The cases with blade tip partly going out of water were also performed. The regular waves did not have significant influences on average loads and power output in the present experiments, but caused large amplitude of the cyclic variation of the loads. The amplitudes of the cyclic load were proved to be

*Address all correspondence to this author.

proportional to the incident wave height, and to be sensitive to the wave frequency and submergence of the rotor. As the tidal turbine getting close to free surface, significant waves were induced by the underwater rotating blade. The effects of surface waves and submergence need to be taken into account in design.

## INTRODUCTION

Tidal turbines can generate power from ocean current with the advantages of high predictability, high energy density, and limited environmental impacts. The concept of extracting power from ocean tides has a long history [1]. With the growing energy demand, tidal turbines have gained increased attention. In many parts of the world, tidal power presents an advantageous resource. About 61.3 TWh/year of tidal current energy technically is available in China. In the East China Sea, some excellent channels are most promising with energy density over $20\,\mathrm{kW\,m^{-2}}$ [2]. In the UK, the extractable resource was estimated to be up to 18 TWh/year [3].

Unsteady hydrodynamic conditions, such as turbulent inflow or free surface waves, would induce more complex loads on the submerged tidal turbines. Surface waves which can penetrate the water column to a depth of half of the wave length is an important part of the unsteady hydrodynamic loads. However the cyclic wave conditions are not considered in standard design procedure of tidal turbines. Tidal turbines nowadays are designed with an increasing size to produce more power from the whole cross-section of the channel. The oscillating wave loads will undoubtedly not only lead to increase of the extreme loads but also accelerate fatigue of the rotor and blades. As tidal turbines getting close to free surface to capture more energy, the dynamic effects on the loads and performance arise from the interaction between tidal turbines and free surface. On one hand, the presence of free surface would affect the power production of tidal turbines. On the other hand, the wake behind the turbine would induce waves and vortex on free surface in turn. The induced waves and vortex may bring safety issues to the nearby ships and structures. As tidal turbines are expected to produce power in the most energetic waters, further studies should be carried out to assess the effects of unsteady loads and free surface.

Only a few experiments have been carried out to study the surface wave effect on tidal turbines. Barltrop et al. [4] performed experiments using a 400 mm diameter rotor in a towing tank with the presence of regular waves. The average thrust and torque were found to be independent with the wave frequencies or wave heights. However significant cyclic variation of the thrust and torque were observed. Similar model tests in towing tanks were reported by Lust et al. [5] and Luznik et al. [6]. They both confirmed that the average thrust and torque was not affected by the waves. Results from Luznik et al. [6] indicated a strong correlation between the measured torque and vertical wave particle velocity. Galloway et al. [3] investigated the effects of waves on an 800 mm 3-bladed horizontal axis TST device, whilst being towed at $0.9\,\mathrm{m\,s^{-1}}$. The regular waves with periods about 2.0 s and heights from 7.5 cm to 15.0 cm at model scale were used in Galloway's experiments. They concluded that the waves caused the significant cyclic loading with the amplitudes of 37% and 35% of the mean for thrust and torque, respectively. Whelan et al. [7] suggested a correction for the effects of free-surface proximity and blockage on the performance of tidal turbines.

The paper presents experiments on a 3-bladed tidal turbine which were performed in a towing tank to contribute to the understanding of the effects of regular waves and free surface on the performance of tidal turbines. Compared to previous studies, a wide range of regular waves with periods from 1.0 s to 3.0 s and heights from 5.0 cm to 15.0 cm at model scale were considered. The submergence of the turbine hub was from 1.0D to 0.45D with an interval of 0.05D (D is the turbine diameter). The cases with blade partly going out of water were firstly reported. The numerical prediction for comparison was made by Guo et al. [8] based on the modified BEM theory with an inclusion of dynamic wake model, added mass and wave excitation forces.

## EXPERIMENT SET-UPS

### Towing Tank

The present experiments were carried out in the towing tank at Zhejiang Ocean University, China. The dimensions of the towing tank are $130\,\mathrm{m} \times 6\,\mathrm{m} \times 3\,\mathrm{m}$. A flap-type wave generator is at the upstream end of the tank. A passive wave-absorbing beach is located at the other end with the damping grids for passive wave dissipation to absorb the wave energy. The carriage velocity is controlled and recorded by the computer. In the present towing test, the carriage velocity was at $0.56\,\mathrm{m\,s^{-1}}$ and $0.68\,\mathrm{m\,s^{-1}}$.

### Test rig

The test rig mainly consisted of an airfoil section tank, a generator/motor, a dynamometer, and a 3-bladed model turbine. The generator/motor was equipped with close-loop controller to ensure precise speed control. The dynamometer was utilized to record the torque and thrust on the shaft.

A 3-bladed tidal turbine as shown in Fig. 1 was used in the present experiments. Compared to marine propellers, the relatively slow rotating speed requires to choosing a larger size rotor for maximizing Reynolds number with moderate towing speed (about $1.0\,\mathrm{m\,s^{-1}}$). Meanwhile, the diameter is limited by blockage of the tunnel and processing difficulty of the aluminum alloy blade. The diameter was chosen to be 800 mm as a compromise to represent a 20 m-diameter, 1 MW prototype tidal turbine in the present experiments. The model blades were considered to be rigid bodies. Froude scaling is the dominant scaling parameter, and the scale ratio is 25. The tidal turbine with relatively low Reynolds number about $0.8 \times 10^5$ (at 75% blade radius) at model

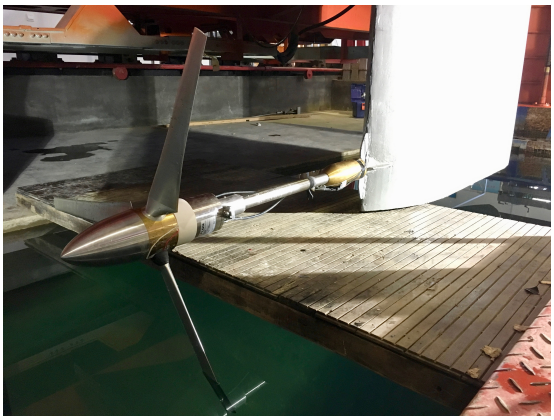

**FIGURE 1**. PHOTO OF THE 1 : 25TH MODEL TURBINE

scale would reduce the unsteady hydrodynamic performance compared to that expected at full-scale with Reynolds number of $1.0 \times 10^6$ [9]. In this paper, all the results from experiments and numerical prediction were shown and discussed at model scale.

The hub diameter is 100 mm, and the blade sections were derived from NACA 63-8xx profile with varying thickness and pre-twist. The span-wise distributions of the chord, pre-twist and thickness are shown in Tab. 1 at model scale.

**TABLE 1**. PARTICULARS OF THE TIDAL TURBINE BLADES AT MODEL SCALE

| $r/R$ | r (mm) | Twist (deg) | Chord (mm) | $t/c$ (%) |
|---|---|---|---|---|
| 0.125 | 50 | 19.5 | 32.0 | 99.9 |
| 0.200 | 80 | 19.5 | 67.9 | 22.0 |
| 0.300 | 120 | 16.5 | 60.7 | 20.0 |
| 0.400 | 160 | 13.3 | 51.9 | 18.3 |
| 0.500 | 200 | 11.6 | 47.6 | 14.8 |
| 0.600 | 240 | 9.4 | 43.3 | 14.2 |
| 0.700 | 280 | 7.3 | 40.1 | 13.6 |
| 0.800 | 320 | 5.2 | 37.6 | 13.1 |
| 0.900 | 360 | 2.7 | 35.3 | 12.5 |
| 1.000 | 400 | 0.0 | 33.2 | 12.0 |

Two wave probes as shown in Fig. 2 were located in front of the tank to record incident waves and wake induced waves. The wave heights at the rotor plane were obtained by changing the phase of the measured incident waves 4.5 m ahead of the rotor. The whole test rig was connected with the main carriage which could move forward in the tank with a constant velocity. Meanwhile the whole test rig could be moved up and down to adjust the submergence of the turbine hub from 0.32 m to 0.96 m in order to satisfy different test conditions. All these mentioned instruments were carefully calibrated before the experiments. All the quantities were recorded with a sampling rate of 100 Hz.

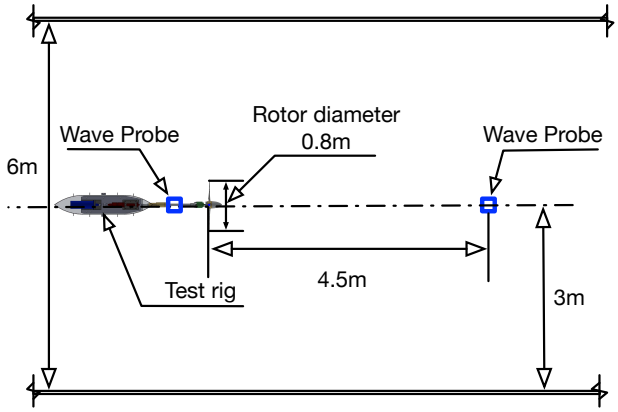


**FIGURE 2**. SCHEMATIC OF THE TEST RIG AND WAVE PROBES ARRANGEMENT.

**TABLE 2**. THE TARGET WAVE PARAMETERS IN CALIBRATION.

| period (s) T | height (cm) H | Length (m) $L_w$ | steepness (%) $\gamma = H/L_w$ |
|---|---|---|---|
| 1.0 | 5.0 | 1.56 | 3.21 |
| 1.2 | 8.0 | 2.25 | 3.56 |
| 1.4 | 8.0 | 3.06 | 2.61 |
| 1.6 | 8.0 | 4.00 | 2.00 |
| 1.6 | 5.0 | 4.00 | 1.25 |
| 1.6 | 8.0 | 4.00 | 2.00 |
| 1.6 | 12.0 | 4.00 | 3.00 |
| 1.8 | 10.0 | 5.06 | 1.98 |
| 2.0 | 10.0 | 6.22 | 1.61 |
| 2.4 | 10.0 | 8.75 | 1.14 |
| 2.8 | 10.0 | 11.38 | 0.88 |
| 3.0 | 10.0 | 12.68 | 0.79 |

## Regular waves

A flap-type wave generator at the upstream end of the towing tank was used to generate regular waves in the present experiments. The typical tidal turbine sites are often located at the channels between the islands near coast. The waves tend to have long periods and relatively small significant heights in these sheltered locations. The periods of the selected regular waves cover a range from 1.0 s to 3.0 s in model scale, with the corresponding range from 5.0 s to 15.0 s in prototype, which are significant for typical tidal turbine sites. These regular waves as shown in Table 2 fall into deep waves and intermediate waves. The wave height was chosen based on a steepness that did not exceed 3.5%.

The reduced frequency and current number are used to describe the degree of unsteadiness caused by the passing waves,

and are given by:

$$k = \frac{\pi f c}{V} \tag{1}$$

$$\mu = \frac{\tilde{u}}{U} \tag{2}$$

where $\tilde{u}$ is the amplitude of the velocity perturbation determined by the passing waves at hub height, $U$ is the mean inflow velocity, $f$ is the physical frequency of the waves, $c$ is blade chord at span-wise position of 75%R, and $V$ is the resultant local inflow velocity seen by the local blade section.

Due to the fact that the depth velocity distribution of the wave particles is not uniform, the wave particle velocity at the hub depth was used in the definition of current number. In the present study, reduced frequency $k$ as shown in Tab. 3 is between 0.02 and 0.04, and current number $\mu$ is under 0.2, ensuring a controllable unsteady inflow.

All the waves have been calibrated before the experiments. The parameters of the calibrated waves are shown in Tab. 2. A fixed wave probe was placed at the center of the towing tank about 50 m away from the upstream wave maker for the wave calibration only. Figure 3 shows the selected time histories of the incident wave elevation with different wave periods.

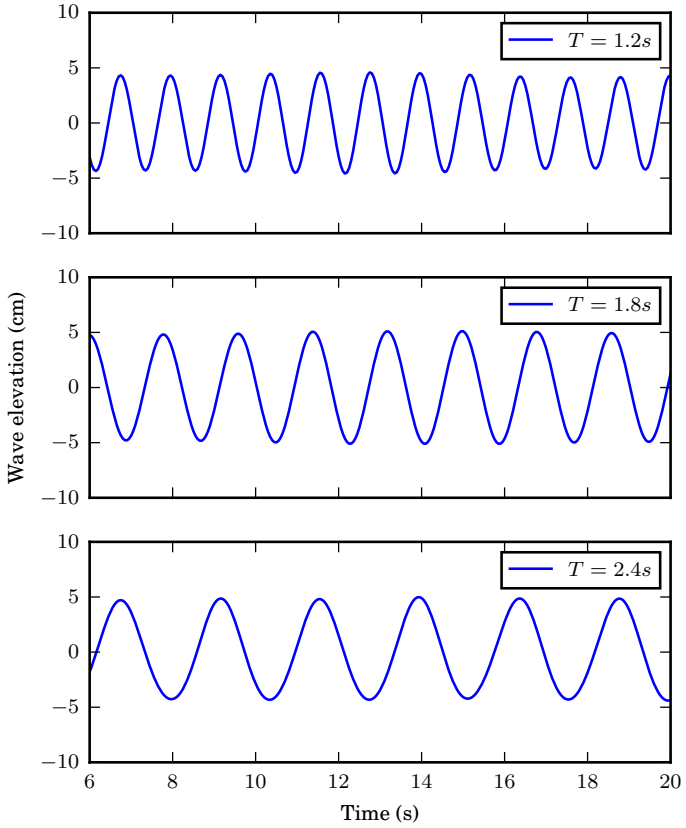


**FIGURE 3**. TIME HISTORIES OF THE WAVE ELEVATION IN CALIBRATION.

## RESULTS AND DISCUSSIONS

### Average power and trust coefficients

The time averaged power coefficient ($C_p$) and thrust coefficient ($C_T$) are presented as a baseline and validation. The $C_p$ and $C_T$ for the cases with and without the presence of waves as a function of the tip speed ratio (TSR) are shown in Figs. 4 and 5. The grey dash line indicates $\pm 5\%$ errors determined by the numerical model. The $C_p$, $C_T$, and TSR are defined as follows:

$$C_p = \frac{M\Omega}{0.5\rho U^3 \pi R^2} \tag{3}$$

$$C_T = \frac{T}{0.5\rho U^2 \pi R^2} \tag{4}$$

$$\text{TSR} = \frac{\Omega R}{U} \tag{5}$$

where $M$ is the measured shaft torque, $T$ is the measured thrust, $\Omega$ is the rotational speed, $U$ is the carriage velocity, $\rho$ is the water density, and $R$ is the rotor radius.

The numerical prediction as comparison and baseline was made by the unsteady BEM code developed by Guo et al. [8]. The numerical prediction was based on the modified BEM model involving dynamic inflow model and dynamic stall model. The added mass effects caused by the unsteady inflow and wave excitation forces on the blades were also included in the numerical prediction. Based on the assumption of slender body, the added mass and wave excitation forces are calculated from the integral of the 2D forces acting along the span-wise blade elements. The rotation of the rotor was simulated by a single degree-of-freedom (DOF) model. The hydrodynamic loads on the rotor from BEM model were used to determine the rotation speed for the next time step. The flow chart of the integral model is illustrated in Fig. 6.

Figures. 4 and 5 show good agreement between the experimental and numerical results. The still water cases (without waves) were performed at the carriage velocity of 0.56 m s$^{-1}$ and 0.68 m s$^{-1}$, and rotor speed from 65 RPM to 138 RPM. The submergence of the turbine hub is 0.64 m (0.8$D$). The cases with the presence of regular waves were performed under the same towing conditions but being exposed to different regular waves. The BEM theory has been proved to be good enough for the steady performance prediction of tidal turbines [6, 10, 11]. At low TSR region ($\lambda < 4$), the rotor was dominated by the stall effects due to large angle of attack with fixed pitch angle. When the TSR was larger than 7, the turbulent wake leaded to the decrease of the power coefficient. The optimal power coefficient was obtained by TSR at 4 to 6. Most of the cases in following were performed in the optimal TSR region.

**TABLE 3**. REDUCED FREQUENCY $k$ AND CURRENT NUMBER $\mu$ OF THE TYPICAL CASES

| Case No. | Waves | | Towing condition | | Reduced frequency | Current number |
|---|---|---|---|---|---|---|
| | T (s) | H (cm) | Submergence (m) | TSR (-) | $k = \pi fc/V$ | $\mu = \tilde{u}/U$ |
| 1 | 1.0 | 5 | 0.64 | 5.4 | 0.044 | 0.018 |
| 2 | 1.2 | 8 | 0.64 | 5.4 | 0.037 | 0.052 |
| 3 | 1.6 | 10 | 0.64 | 5.4 | 0.028 | 0.106 |
| 4 | 2.4 | 10 | 0.64 | 5.4 | 0.018 | 0.127 |
| 5 | 3.0 | 10 | 0.64 | 5.4 | 0.015 | 0.130 |
| 6 | 1.2 | 8 | 0.64 | 4.5 | 0.044 | 0.052 |
| 7 | 1.2 | 8 | 0.64 | 6.0 | 0.033 | 0.052 |
| 8 | 1.2 | 8 | 0.64 | 7.0 | 0.028 | 0.052 |
| 9 | 1.6 | 10 | 0.36 | 5.4 | 0.028 | 0.164 |
| 10 | 1.6 | 10 | 0.56 | 5.4 | 0.028 | 0.120 |
| 11 | 1.6 | 10 | 0.72 | 5.4 | 0.028 | 0.093 |

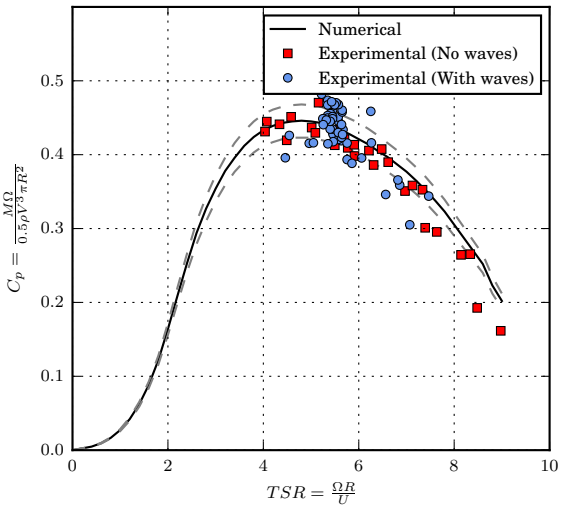


**FIGURE 4**. POWER COEFFICIENT ($C_P$) WITH AND WITHOUT WAVES.

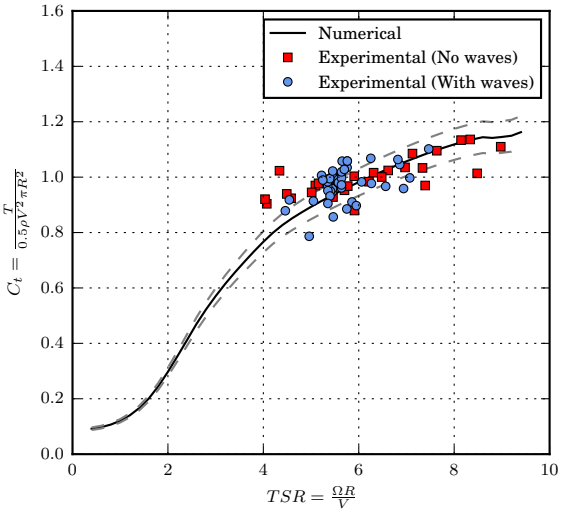


**FIGURE 5**. THRUST COEFFICIENT ($C_P$) WITH AND WITHOUT WAVES.

The Reynolds number at 75% radius was between 0.87-1.52 $\times 10^5$ in the present cases. Although it was still lower than that expected of the prototype tidal turbines, it was at the same level compared to the previous towing model tests [3, 4, 6, 12]. The carriage velocity of 0.56 m s$^{-1}$ and 0.68 m s$^{-1}$ is equivalent to 2.8 m s$^{-1}$ and 3.4 m s$^{-1}$ in full scale respectively, which are the general rated current speed for tidal turbines.

The results from cases with and without the presence of the waves have no significant differences in the $C_p$ and $C_T$ curves, which indicates that the passing waves did not affect the time averaged loads and power output. It was also concluded by some previous studies [3,6,13]. For linear waves, water particles moved as an circle in deep water. The effects of the back and forth wave induced velocities can be canceled out by the average in one wave period. However the passing waves would undoubtedly have influences on the dynamic part of the loads and power output of the tidal turbine.

## The effects of surface waves

The time histories of the measured incident waves and torque are shown in Fig. 7. The typical wave test procedure is presented as follows. The turbine started to rotate at given speed without any forward velocity. As the waves arrive the rotor plane, the carriage speeded up with constant acceleration and then maintained the velocity. Finally, it stopped before the tank end after more than 25 wave periods.

The measured torque can be decomposed into the static part and wave induced dynamic part. From the power coefficient curves, we know that the average torque was not influenced by

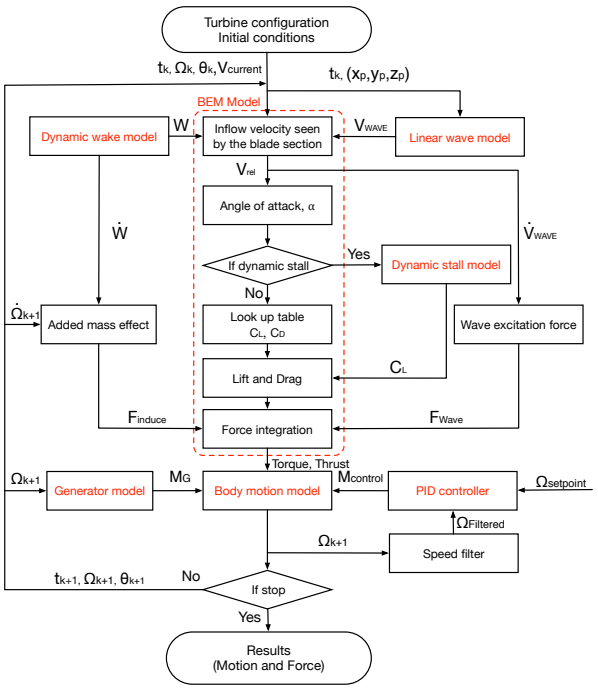


**FIGURE 6**. THE FLOW CHART OF THE INTEGRAL NUMERICAL MODEL. [8]

the passing waves. The main effects caused by the passing waves were the cyclic oscillation of the torque (Fig. 7 (d)). The average amplitude of the cyclic torque was defined as $M^{wave}$. The $M^{wave}$ as a function of wave height is shown in Fig. 8, and as a function of the instantaneous current number is shown in Fig. 9.

Due to the linear relation between the wave heights and the range of the cyclic torque $M^{\mathrm{WAVE}}$ as shown in Fig. 8, the effect caused by the wave heights could be neglected. The slope of the lines, or known as load transfer function $k_M$ (dynamic loads induced by a unit wave height), can be introduced to estimate the effects of waves as follows:

$$k_M = \frac{\Delta M^{\mathrm{WAVE}}}{\Delta H^{\mathrm{WAVE}}} \tag{6}$$

The amplitudes of the dynamic torque normalized by the mean value as a function of the instantaneous current number show that a small disturbance of the inflow could induce large amplitude of the cyclic variation (about 50% of the mean load). It also indicates that the waves and its effects on the torque are in phase. When the wave elevation at the rotor plane reached the highest level, the wave particle had maximum forward speed, and therefore it caused the maximum loads on the rotor, and vice versa. It also indicated that the dynamic effects was small and could be neglected due to relatively small incident linear waves.

The $k_M$ as a function of the wave frequency are shown in

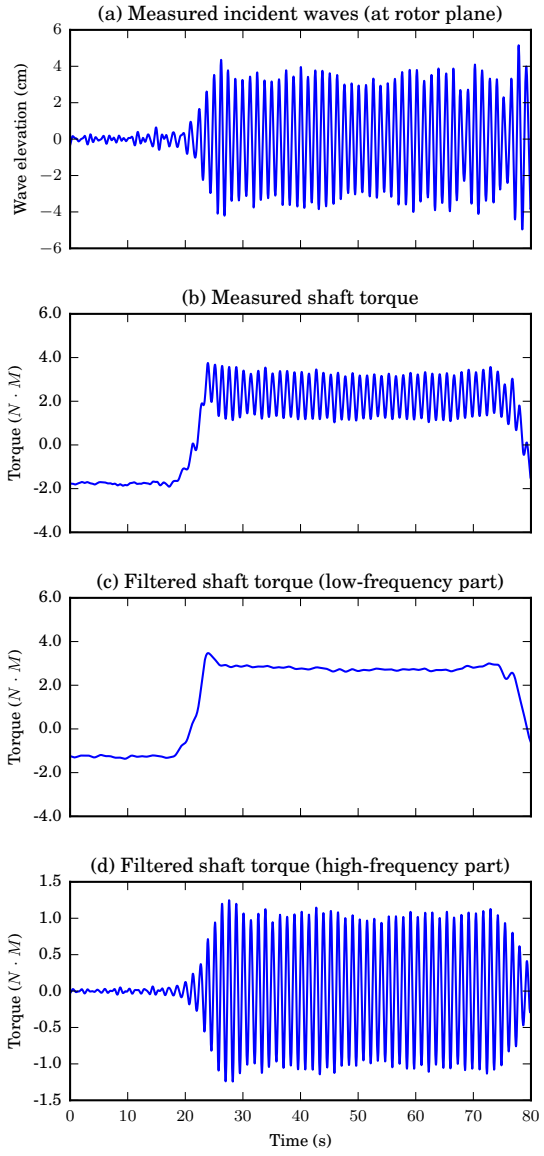


**FIGURE 7**. THE TIME HISTORIES OF THE MEASURED INCIDENT WAVES AND TORQUE, FOR $U = 0.68\,\mathrm{m\,s^{-1}}$, ROTATIONAL SPEED f = 1.89Hz, SUBMERGENCE RATIO $H/D = 0.8$ AND INCIDENT WAVE PERIOD $T = 1.6$S, $H = 8$CM.

Fig. 10. For short waves ($f > 2.0$Hz), the effect of waves are restricted in the limited depth, and it cannot have a significant influences on the tidal turbine. In this wave frequency region, the $k_M$ are very small, and can be neglected. For intermediate waves, the effect of submergence become more important. When the submergence ratio $H/D = 0.6$, a resonant peak around $f = 0.6$ can be identified. For the cases with $H/D = 0.8$, the $k_M$ increases from zero to the quasi-static value with the decreasing wave frequency. To avoid severe wave loads on tidal turbines, the submergence of the hub should be at least 0.8 of the rotor

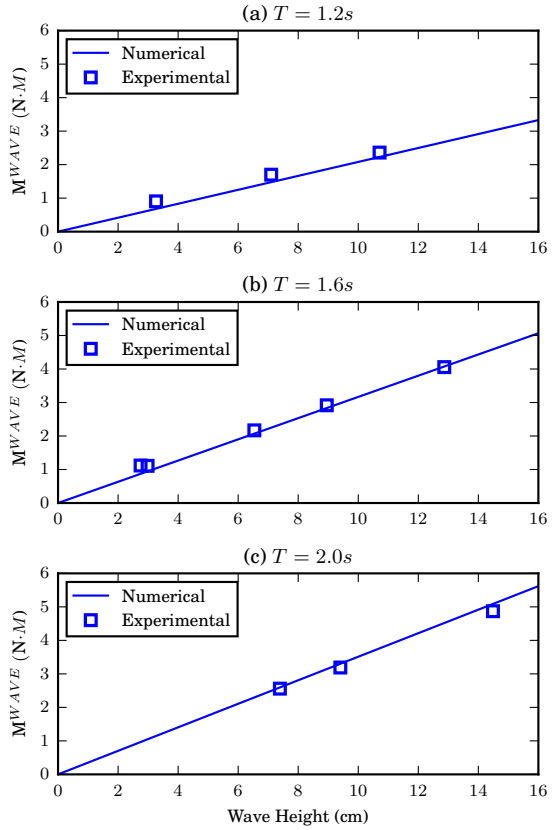


**FIGURE 8**. THE WAVE INDUCED TORQUE RANGE $M^{WAVE}$ AS A FUNCTION OF THE WAVE HEIGHT.

diameter. For long waves, the water particles have almost the same velocities throughout the whole water column. The submergence is not the key factor any more. The $k_M$ tends towards the same value for different submergences. The fixed $k_M$ caused by the long waves is independent with submergence, which can be used as an approximate way for the wave load prediction.

## The effects of free surface

The cases with different submergence ratio from 0.45 to 1.0 were performed. For the cases without the presence of waves, the time averaged power coefficients as a function of submergence ratio are shown in Fig. 11. The free surface limit of the hub submergence ($H/D = 0.5$) means that the blade tip is at the free surface. The cases with blade tip partly going out of water were also performed ($H/D = 0.45$). With the closing distance between the blade tip and free surface, the $C_p$ were observed to be a constant with different TSRs. When the blade partly going out of water, a slight loss of the power coefficient can be seen from the $C_p$ curves in Fig. 11.

The effect of intermediate waves on torque was proved to be sensitive to submergence in Fig. 10. Two waves with frequencies $f = 0.833$Hz and 0.625Hz were selected to investigate the

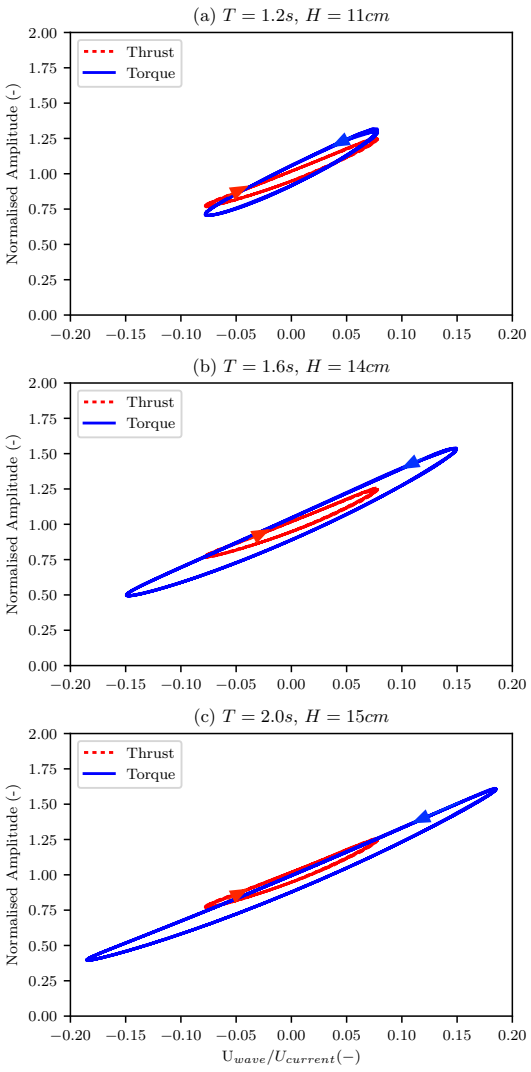


**FIGURE 9**. THE DYNAMIC TORQUE NOMORLIZED BY THE MEAN AS A FUNCTION OF THE INSTANTANEOUS CURRENT NUMBER.

effects of the submergence. The load transfer functions $k_M$ as a function of submergence ratio $H/D$ are shown in Fig. 12. When the submergence ratio is larger than 0.7, the linear numerical model agreed well with the experimental results. With the turbine getting close to the free surface, the wave particle velocity increase shapely. When $H/D < 0.6$, the numerical model obviously underestimated the wave induced loads. In this situation, the maximum horizontal wave particle velocity at the blade tip could be larger than 50% of the inflow current velocity, which means that regarding the water particle velocity as a disturbance of the mean current velocity in the numerical model is no longer suitable. The dynamic wake behind the rotor was also strongly affected by the free surface. To make the numerical prediction more precise,

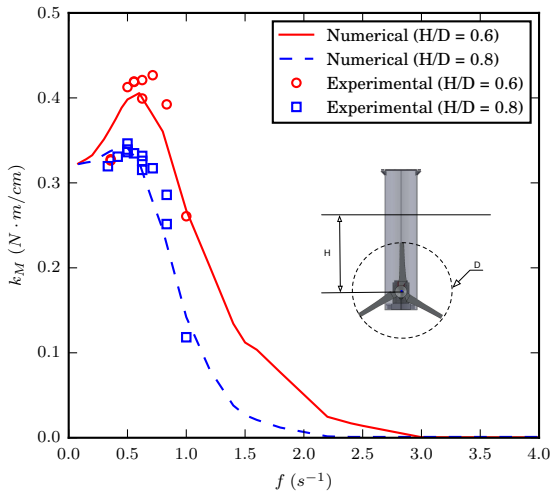


**FIGURE 10**. $k_M$ AS A FUNCTION OF WAVE FREQUENCY ($T^{-1}$) WITH DIFFERENCE SUBMERGENCE RATIO.

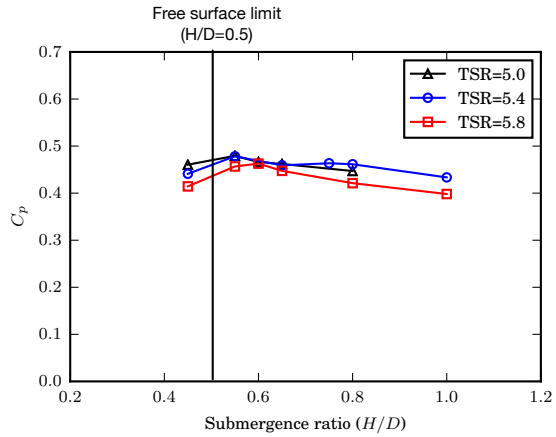


**FIGURE 11**. $C_p$ AS A FUNCTION OF SUBMERGENCE RATIO ($H/D$).

more details about the free surface should be taken into account. To avoid severe wave loads on tidal turbines, the submergence of the hub should be at least 0.8 of the rotor diameter.

### Wake induced waves

As the tidal turbine getting close to free surface, significant waves was induced by the rotor. The captured induced waves for $U = 0.68\,\mathrm{m\,s^{-1}}$, rotational speed f = 1.35Hz and submergence ratio $H/D = 0.55$ as an example and $H/D = 1.0$ for comparison are shown in Fig. 13. The time histories recorded by the wave probe behind the rotor plane is shown in Fig. 15 for the same cases. By performing the FFT transform, the frequency features of the induced waves are shown in Fig. 15. Several frequency peaks can be identified. The fundamental frequency is 1.35 Hz, which is equal to the rotational frequency. Twice, three and four

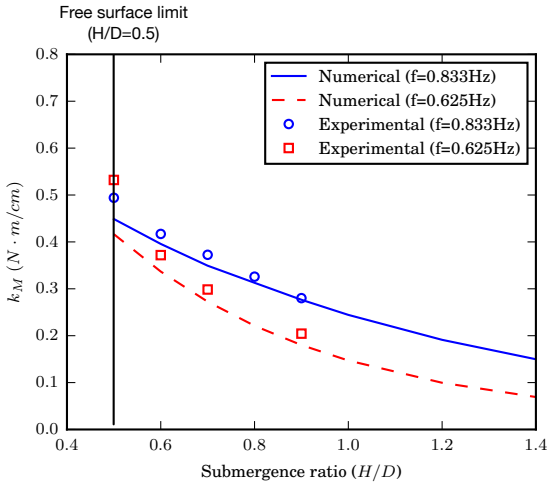


**FIGURE 12**. $k_M$ AS A FUNCTION OF SUBMERGENCE RATIO ($H/D$).

times of the base frequency were also observed. With the smaller submergence ratio, the amplitudes of the induced waves became larger, and the higher order parts were also more significant. When the blade tip partly going-out-of water, more complex impacts were observed between the blade tip and free surface. Except for the induced waves, significant vortex shedding by the blade tip occurred in the wake as shown in Fig. 14.

A primary explanation of the induced waves could be that it was caused by the interaction between the shedding tip vortex and the free surface. The rotor induce waves and vortex had a large influence region in the downstream, which would bring safety issues to the nearby ships and structures. Further study about the characteristics and mechanics of the interaction between the underwater rotor and free surface are needed, and will be the future work for the authors.

## CONCLUSIONS

The present experiments on a three bladed tidal turbine is to contribute to the understanding of the effects of submergence and free surface waves on tidal turbines. The cases with and without the surface waves were performed in a towing tank. Some conclusions are summarized as follows.

The presence of regular waves and free surface did not affect the average loads and power output from the present experimental observation. A small disturbance of the inflow caused by the passing waves (15% of the mean velocity) could induce large amplitude of the cyclic variation of the loads on the rotor (50% of the mean load).

For linear incident waves, amplitude of the cyclic loads on the rotor was proportional to wave heights. The load transfer function $k_M$ defined by the dynamic torque caused by a unit wave height as a function of wave frequency were introduced for estimating

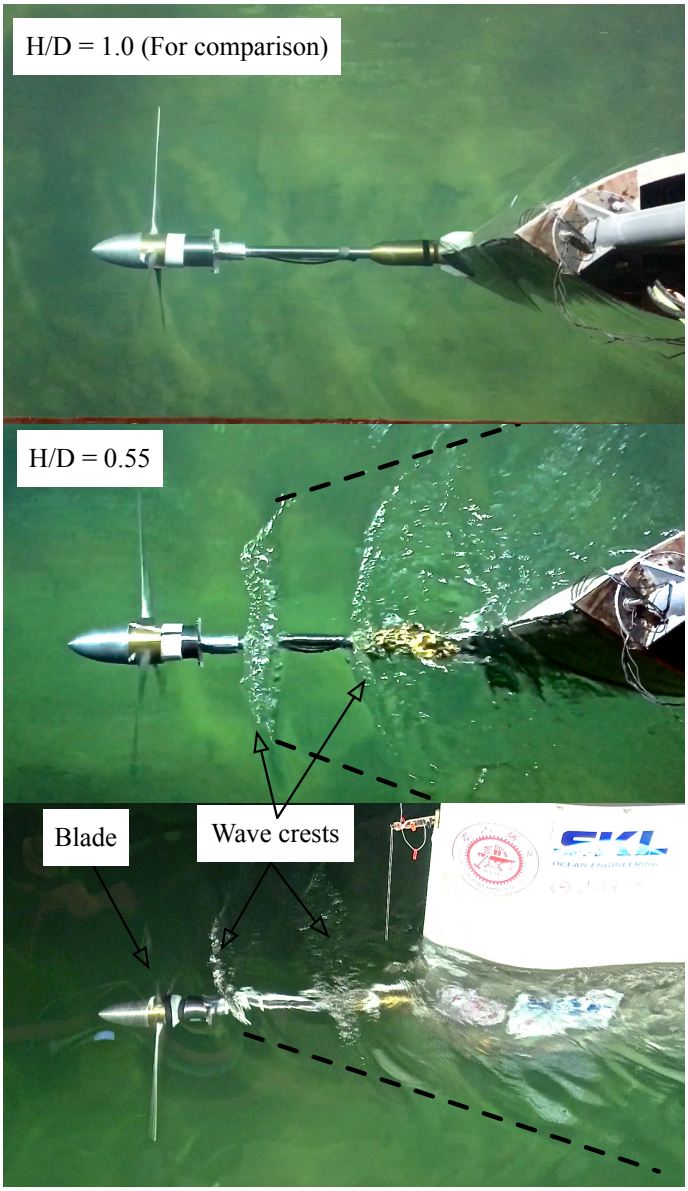


**FIGURE 13**. THE WAKE INDUCED WAVES BEHIND THE ROTOR FOR $U = 0.68\,\mathrm{m\,s^{-1}}$, ROTATIONAL SPEED f = 1.35Hz AND SUBMERGENCE RATIO $H/D = 0.55$.

of the cyclic wave loads. The $k_M$ was proved to be sensitive to submergence and wave frequency. To avoid severe wave load effects, submergence should be at least 0.8 of the rotor diameter.

As tidal turbine getting close to the free surface, significant waves induced by the underwater blade could be observed. By performing the FFT transform on the recorded time series, the amplitude spectrum of the induced waves was obtained. The fundamental frequency of the induced waves was equal to the rotational frequency of the rotor. Several higher order frequency peaks were identified. For the cases with blade tip partly going

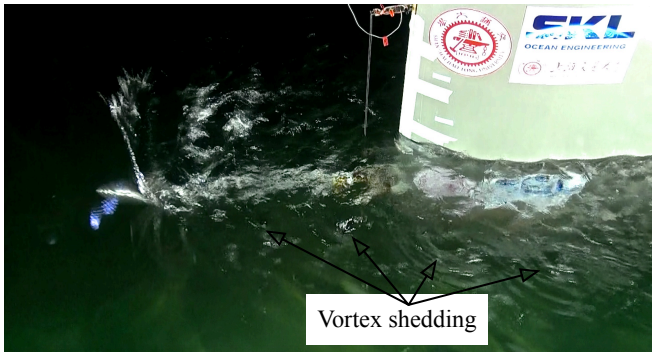


**FIGURE 14**. THE TIP VORTEX SHEDDING BEHIND THE ROTOR (BLADE TIP OUT OF WATER).

out of water, vortex shedding from the blade tip can be seen. The induced waves and vortex shedding by tidal turbines may bring safety issues to the nearby ships and structures, which need to be paid attention in design.

## ACKNOWLEDGMENT

The authors thank Dr. Handi Wei, Xiaona Ge, and Peng Zhu for their contributions in the experiments. The present study is funded by the National Natural Science Foundation of China (Grant No. 51679137) and the Open Project of the State Key Laboratory of Ocean Engineering (Grant No. GKZD010068). Zhejiang Ocean University also provided much support. All of the help is acknowledged by the authors. The first author also acknowledges the support of the China Scholarship Council.

## REFERENCES

[1] Elghali, S. B., Benbouzid, M., and Charpentier, J. F., 2007. "Marine tidal current electric power generation technology: State of the art and current status". In 2007 IEEE International Electric Machines & Drives Conference, Vol. 2, IEEE, pp. 1407–1412.

[2] Liu, H., Ma, S., Li, W., Gu, H., Lin, Y., and Sun, X., 2011. "A review on the development of tidal current energy in china". *Renewable and Sustainable Energy Reviews,* ***15***(2), pp. 1141–1146.

[3] Galloway, P. W., Myers, L. E., and Bahaj, A. S., 2014. "Quantifying wave and yaw effects on a scale tidal stream turbine". *Renewable Energy,* ***63***, pp. 297–307.

[4] Barltrop, N., Varyani, K., Grant, A., Clelland, D., and Pham, X., 2007. "Investigation into wavecurrent interactions in marine current turbines". *Proceedings of the Institution of Mechanical Engineers, Part A: Journal of Power and Energy,* ***221***(2), pp. 233–242.

[5] Lust, E. E., Luznik, L., Flack, K. A., Walker, J. M., and Benthem, M. C. V., 2013. "The influence of surface gravity

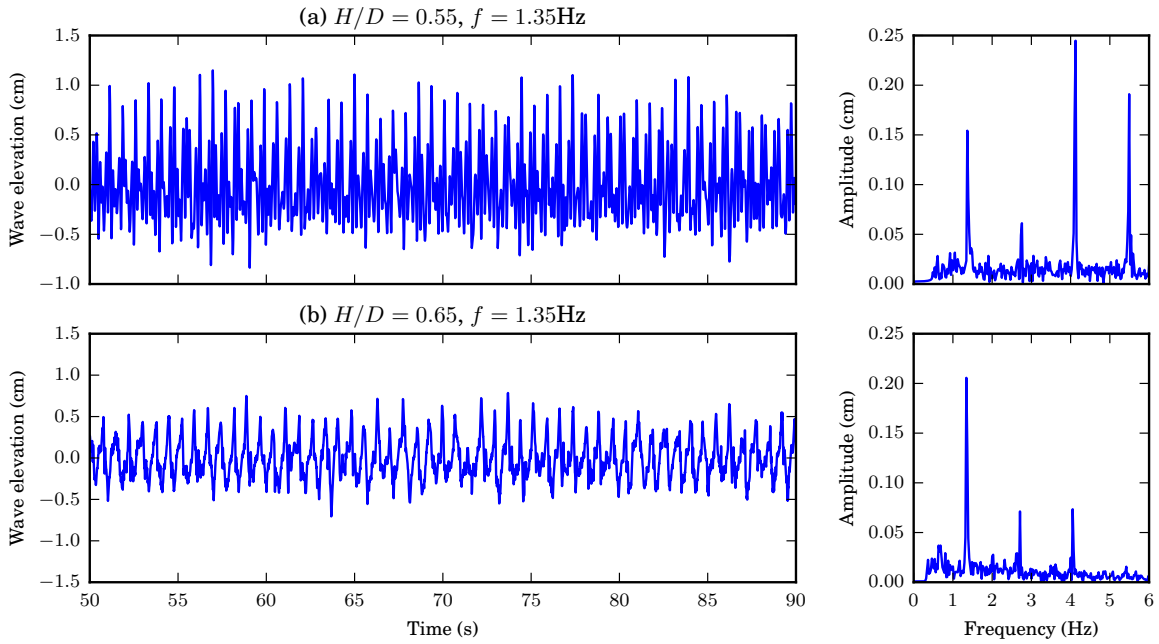


**FIGURE 15**. THE TIME HISTORIES AND AMPLITUDE SPECTRUMS OF THE INDUCED WAVES FOR $U = 0.68\,\mathrm{m\,s^{-1}}$, ROTATIONAL SPEED f = 1.35Hz AND SUBMERGENCE RATIOS $H/D = 0.55$ and $H/D = 0.65$.


waves on marine current turbine performance". *International Journal of Marine Energy,* ***34***, pp. 27 – 40. Special Issue Selected Papers - EWTEC2013.

[6] Luznik, L., Flack, K. A., Lust, E. E., and Taylor, K., 2013. "The effect of surface waves on the performance characteristics of a model tidal turbine". *Renewable Energy,* ***58***, pp. 108–114.

[7] Whelan, J., Graham, J., and Peiro, J., 2009. "A free-surface and blockage correction for tidal turbines". *Journal of Fluid Mechanics,* ***624***, pp. 281–291.

[8] Guo, X., Yang, J., Gao, Z., Moan, T., and Lu, h., 2017. "The surface wave effects on the performance and the loading of a tidal turbine". *Submitted to Renewable Energy*.

[9] Shyy, W., Lian, Y., Tang, J., Viieru, D., and Liu, H., 2007. *Aerodynamics of low Reynolds number flyers*, Vol. 22. Cambridge University Press.

[10] Molland, A. F., Bahaj, A. S., Chaplin, J. R., and Batten, W. M. J., 2004. "Measurements and predictions of forces, pressures and cavitation on 2-d sections suitable for marine current turbines". *Proceedings of the Institution of Mechanical Engineers, Part M (Journal of Engineering for the Maritime Environment),* ***218***(M2), pp. 127–38.

[11] Bahaj, A. S., Molland, A. F., Chaplin, J. R., and Batten, W. M. J., 2007. "Power and thrust measurements of marine current turbines under various hydrodynamic flow conditions in a cavitation tunnel and a towing tank". *Renewable Energy,* ***32***(3), pp. 407–426.

[12] Milne, I., Day, A., Sharma, R., and Flay, R., 2015. "Blade loading on tidal turbines for uniform unsteady flow". *Renewable Energy,* ***77***, pp. 338–350.

[13] Faudot, C., and Dahlhaug, O. G., 2012. "Prediction of wave loads on tidal turbine blades". *Energy Procedia,* ***20***, pp. 116–133.